INTERNATIONAL JOURNAL FOR NUMERICAL METHODS IN FLUIDS
*Int. J. Numer. Meth. Fluids* 2005; **47**:971–977
Published online 29 December 2004 in Wiley InterScience (www.interscience.wiley.com). DOI: 10.1002/fld.882

# Large eddy simulation of compressible turbulence using high-resolution methods

M. Hahn and D. Drikakis*,†

*School of Engineering, Aerospace Sciences, Fluid Mechanics and Computational Science Group, Cranfield University, Cranfield, Bedfordshire, MK43 0AL, U.K.*

SUMMARY

The paper presents a numerical investigation of high-resolution schemes for solving the compressible Euler and Navier–Stokes equations in the context of implicit large eddy simulation (ILES), also known as monotone integrated LES (MILES). We have employed three high-resolution schemes: a flux vector splitting (FVS), a characteristics-based (Godunov-type) and a hybrid total variation diminishing (TVD) scheme; and carried out computations of: (i) decaying turbulence in a triply periodic cube and (ii) compressible flow around open cavities for low and high Reynolds numbers, at transonic and supersonic speeds. The decaying turbulence simulations show that all high-resolution schemes employed here provide plausible solutions without adding explicit dissipation with the energy spectra being dependent on the numerics. Furthermore, the ILES results for cavity flows agree well with previously published direct numerical simulations and experimental data. Copyright © 2004 John Wiley & Sons, Ltd.

KEY WORDS: compressible flows; large eddy simulation; high-resolution methods; turbulence

## 1. INTRODUCTION

It has been observed for more than a decade that high-resolution methods have characteristics that mimic the effects of finite viscosity and thermal conductivity and lead to a ‘dissipation’ which is similar to that achieved by adequately resolved numerics involving finite Reynolds and Prandtl numbers [1–13].

These methods are currently used to simulate a broad variety of complex flows, e.g. flows that are dominated by vorticity leading to turbulence, flows featuring shock waves and turbulence, and the mixing of materials. Such flows are extremely difficult to practically obtain

*Correspondence to: Dimitris Drikakis, School of Engineering, Aerospace Sciences, Fluid Mechanics and Computational Science Group, Cranfield University, MK43 0AL, Cranfield, U.K.
†E-mail: d.drikakis@cranfield.ac.uk

Contract/grant sponsor: EPSRC
Contract/grant sponsor: BAE SYSTEMS
Contract/grant sponsor: MoD

*Received 27 April 2004*
*Revised 29 July 2004*
*Accepted 9 August 2004*

stably and accurately in under-resolved conditions (with respect to grid resolution) using classical linear, both second- and higher-order accurate schemes.

Recently, there has been an increasing interest in investigating high-resolution methods in a variety of turbulent flow computations, see Reference [12] for a recent review. The success of high-resolution methods to compute turbulent flows seems to depend on a delicate balance of truncation errors due to wave-speed-dependent terms (chiefly responsible for numerical dissipation) in the case of Godunov-type methods and hyperbolic part of the flux. It is the essence of this balance that needs to be understood. Results from the implementation of high-resolution methods in wall-bounded flows [9, 12] show that in principle there is nothing that prevents the use of these methods in near wall flows even without using an explicit turbulence model. Both ILES and classical LES based on an explicit subgrid scale (SGS) turbulence modelling pose substantial challenges in high-Reynolds, near-wall flows, especially in the presence of separation from gently curved surfaces, where resolution and thus computing-cost issues are critical.

In the present study, we investigate the limits of the ILES approach in the context of under-resolved—grid-size bias—simulations, using different high-resolution schemes. Results are presented from numerical experiments for decaying turbulence in a triply periodic cube and compressible, open cavity flows at transonic and supersonic speeds.

## 2. NUMERICAL FRAMEWORK

The physics of (Newtonian) fluid flow is governed by the Navier–Stokes equations. These equations can be solved by considering the coupled generalized conservation laws namely the continuity, momentum and energy equations

$$\frac{\partial \rho}{\partial t} + \nabla \cdot (\rho \mathbf{u}) = 0 \tag{1}$$

$$\frac{\partial \rho \mathbf{u}}{\partial t} + \nabla \cdot (\rho \mathbf{u}\mathbf{u}) = -\nabla \cdot \mathbf{P} \tag{2}$$

$$\frac{\partial e}{\partial t} + \nabla \cdot (e\mathbf{u}) = -\nabla \cdot (\mathbf{u} \cdot \mathbf{P}) - \nabla \cdot \mathbf{q} \tag{3}$$

where $\mathbf{u}$, $\rho$, $e$, and $\mathbf{q}$ stand for the velocity components, density, total energy per unit volume, and heat flux, respectively. The tensor $\mathbf{P}$ for a Newtonian fluid is defined by $\mathbf{P} = p(\rho, T)\mathbf{I} + \frac{2}{3}\mu(\nabla \cdot \mathbf{u})\mathbf{I} - \mu[(\nabla \mathbf{u}) + (\nabla \mathbf{u})^{\mathrm{T}}]$, where $p(\rho, T)$ is the scalar pressure, $\mathbf{I}$ is the identity tensor, $T$ is the temperature, and $\mu$ is the dynamic viscosity coefficient. The above system is completed by an equation of state. For a perfect gas the equation of state is given by $p = \rho RT$, where $R$ is the gas constant.

For the solution of Equations (1)–(3), we have employed an explicit, third-order TVD Runge–Kutta scheme [14], central differences for the viscous terms and three high-resolution schemes for the discretization of the advective terms. These schemes are briefly described below (for further details see References [15, 16]) for the one-dimensional, inviscid counterpart of the equations in matrix form $\partial \mathbf{U}/\partial t + \partial \mathbf{E}/\partial x = 0$, where $\mathbf{U}$ is the array of the unknown variables and $\mathbf{E}$ is the flux associated with the terms in $x$-direction. The advective flux derivative

 

$\partial \mathbf{E}/\partial x$ (similarly, for the other advective flux derivatives) is discretized at the centre of the control volume (i) using the values of the intercell fluxes, i.e. $\partial \mathbf{E}/\partial x = (\mathbf{E}_{i+1/2} - \mathbf{E}_{i-1/2})/\Delta x$. The definition of the intercell flux function distinguishes among the different high-resolution schemes employed here.

The FVS scheme defines the intercell advective flux as $\mathbf{E}^{\text{SW-FVS}}_{i+1/2} = \mathbf{E}^{+}_{i+1/2}(\mathbf{U}_{\text{L}}) + \mathbf{E}^{-}_{i+1/2}(\mathbf{U}_{\text{R}})$, where the left, $\mathbf{U}_{\text{L}}$, and right, $\mathbf{U}_{\text{R}}$, states of the conservative variables can be obtained by first-, second- or higher-order accurate interpolation schemes. Here, the positive and negative fluxes are computed by an improved version of the Steger–Warming FVS (SW-FVS) scheme [15, 16] in conjunction with first-order interpolation for $\mathbf{U}_{\text{L}}$ and $\mathbf{U}_{\text{R}}$. The first-order interpolation was selected in order to provide a dissipative numerical scheme that can be compared against less dissipative options as described below.

The characteristics-based (averaging) scheme [17] is a Godunov-type method that defines the conservative variables along the characteristics as functions of their characteristic values. A third-order interpolation scheme [15] has been used here to compute the characteristic values from the left or right states depending on the sign of the characteristic speed (eigenvalues). The scheme is third-order accurate in both space and time when it is used in conjunction with a third-order TVD Runge–Kutta scheme for the time integration. The hybrid TVD scheme defines the advective flux as

$$\mathbf{E}_{i+1/2} = \psi_{i+1/2}\mathbf{E}^{(\text{SW-FVS})}_{i+1/2} + (1 - \psi_{i+1/2})\mathbf{E}^{\text{CB}}_{i+1/2}$$

where $\mathbf{E}^{(\text{SW-FVS})}_{i+1/2}$ and $\mathbf{E}^{\text{CB}}_{i+1/2}$ are the intercell fluxes according to the SW-FVS and characteristics-based schemes, which are used in conjunction with first- and third-order interpolation schemes, respectively (see References [15, 16] for details). The term $\psi_{i+1/2}$ is a limiter function defined by the square of the (local) Mach number differences across cell faces [15].

Limiters are the general non-linear mechanism that distinguishes modern methods from classical linear schemes. Their role is to act as a non-linear switch between more than one underlying linear method thus adapting the choice of numerical method based upon the behaviour of the local solution. Limiters result in non-linear methods even for linear equations in order to achieve second-order accuracy simultaneously with monotonicity. Numerical flux limiters can act like dynamic, self-adjusting models, modifying the numerical viscosity to produce a non-linear eddy viscosity [5, 9, 12].

## 3. RESULTS

### *3.1. Decaying turbulence in a triply periodic cube*

ILES of homogeneous decaying turbulence has been carried out in a three-dimensional cube applying periodic boundary condition in each spatial direction. The same case has been employed by other researchers for diagnosing ILES [7, 9, 11]. The compressible Euler equations have been employed on uniformly spaced grids of three different resolutions $32^3$, $64^3$, and $128^3$ with initial conditions as described by Herring and Kerr [18, p. 2793]. The analysis of the computational results has been performed by transforming the kinetic energy into Fourier space via a power spectrum estimation. The energy spectra (ES) using the characteristics-based (Godunov-type) scheme are shown in Figure 1 at dimensionless time $t = 1.07$; $t = l_{\text{o}}/u_{\text{o}}$; $l_{\text{o}}$ is the length of the box and $u_{\text{o}}$ is chosen to satisfy $e_{\text{o}} = \rho_{\text{o}} u_{\text{o}}^2$, where $e_{\text{o}}$ and $\rho_{\text{o}}$ are the reference

 

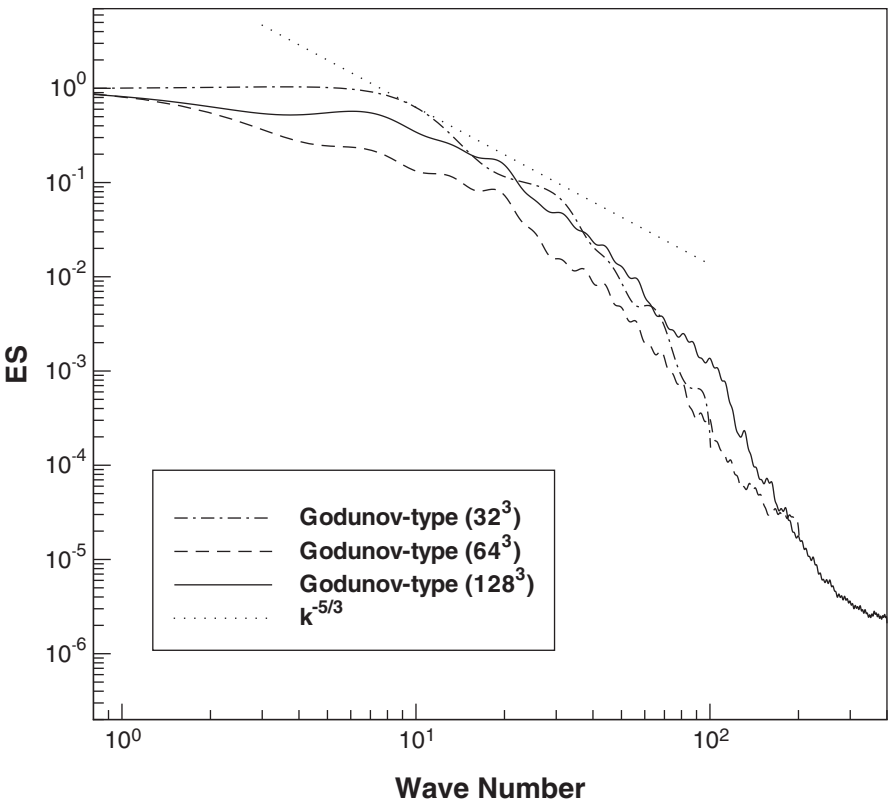


Figure 1. Grid resolution studies using the characteristics-based (Godunov-type) scheme.

(total) energy and density, respectively, corresponding to Mach number $M = 0.1$. We note that separation of solenoidal and non-solenoidal components in the spectral analysis, as suggested in References [4, 19], is required at higher Mach numbers, but at $M = 0.1$ compressibility effects are small. For the different grid resolutions (Figure 1), we observe separation of the energy spectra at both small and large scales. At wave numbers between 8 and 30 the energy spectra approach Kolmogorov's $k^{-5/3}$ slope and decline more rapidly at higher wave numbers (smaller scales) due to numerical dissipation.

A comparison of the simulation results using different high-resolution schemes on the $128^3$ grid is presented in Figure 2. All schemes produce plausible solutions without resorting to explicit addition of dissipation (e.g. through SGS modelling), but the computations reveal the dependence of the results on the schemes' details. The FVS and hybrid TVD schemes are more dissipative, thus, leading to a sharper decrease in energy at wave numbers higher than 26. The FVS contribution to the hybrid flux accounts for about 40% of the total flux value.

### *3.2. Open cavity flows*

Compressible, turbulent flow past an open cavity encompasses a variety of flow phenomena including large and small vortical structures, free shear layers, transitional flow, flow separation

 

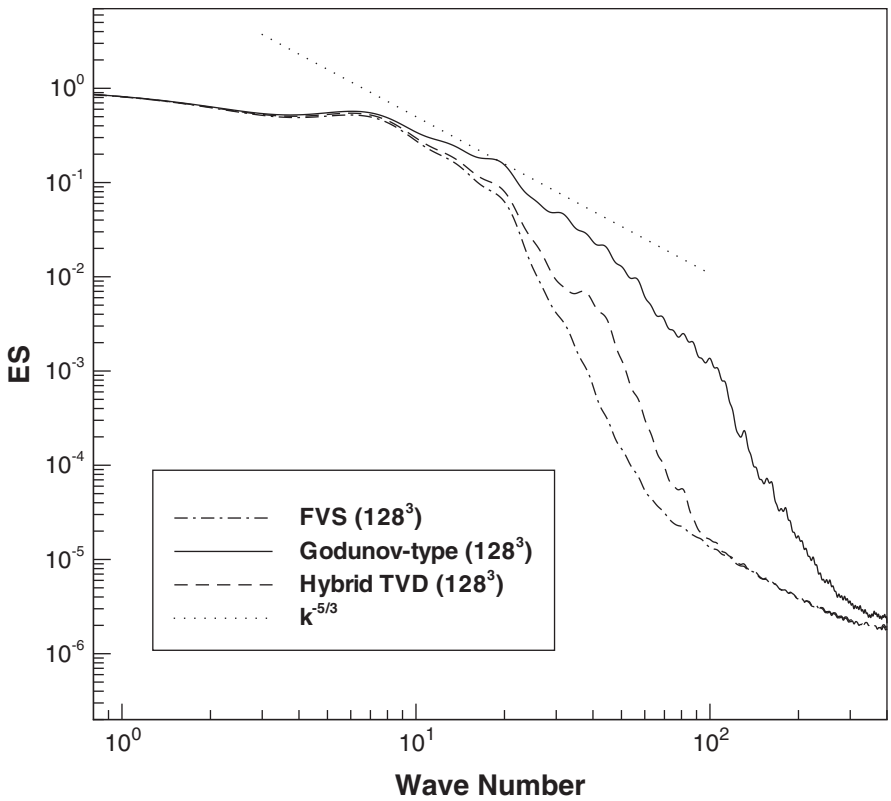


Figure 2. Results using different high-resolution schemes on a $128^3$ grid.

and flow re-laminarization, shock and rarefaction waves. DNS studies were performed in Reference [20] at low Reynolds numbers to investigate the resonant instabilities in the flow past an open, rectangular cavity.[‡] Further, experimental (and computational) results for cavity flows at high Reynolds numbers and supersonic speeds have been presented in Reference [21].

In this study, we have carried out under-resolved simulations for a broad range of transonic and supersonic open cavity flows using the hybrid TVD and characteristics-based (Godunov-type) schemes and compared the results against the aforementioned experimental and DNS data. In the DNS of Reference [20] the grid resolution was 15 times finer than in the present ILES studies. The characteristics-based scheme was found to provide less dissipative solutions for the transonic cases. For the supersonic case the hybrid TVD scheme was preferred due to its more dissipative properties. Instantaneous snapshots of the two-dimensional flow at $M_\infty = 0.8$ and $Re = 1.813 \times 10^5$ are depicted in Figure 3. Cavity resonance arises from a pressure feedback loop including shear layer instability, separation at the leading edge, vortical structures, noise radiation at the trailing edge and re-attachment.

[‡]The Reynolds number is $Re = 2500$ based on the cavity depth and free stream velocity, which is equivalent to $Re = 56.8$ based on the momentum thickness at the cavity's leading edge.

 

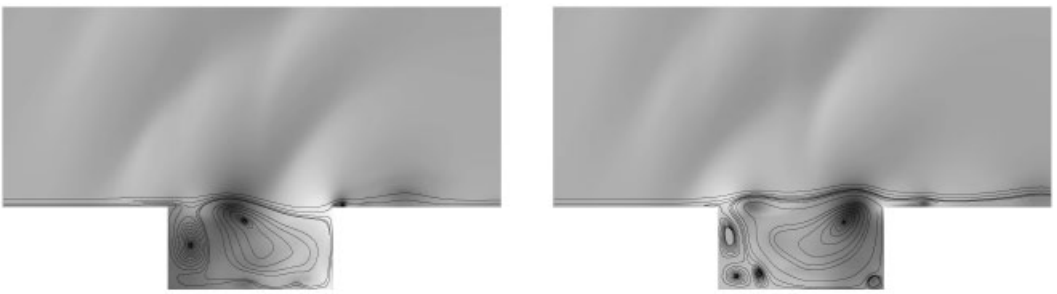

Figure 3. Iso-density contours and streamlines at two different time instants for the transonic cavity flow at $M_\infty = 0.8$ and $Re = 1.813 \times 10^5$.

Table I. Strouhal number comparisons of ILES with DNS [20] and experimental data [21]. The *Re* number is based on the cavity's depth and free stream velocity.

| Mach number | Reynolds number | ILES | DNS | Experiment |
|---|---|---|---|---|
| 0.5 | $2.5 \times 10^3$ | 0.730 | 0.74 | |
| 0.6 | $2.5 \times 10^3$ | 0.683 | 0.70 | |
| 0.8 | $2.5 \times 10^3$ | 0.635 | 0.65 | |
| 1.5 | $4.5 \times 10^5$ | 0.197 | | 0.208 |

Table I shows results for the Strouhal number as predicted by the present ILES, DNS of Reference [20] for transonic flows (at low Reynolds numbers) and experimental data of Reference [21] for supersonic flow at high Reynolds number. The comparison of dominant frequencies shows the applicability of ILES for open cavity flows. Simulations for the transonic cases using a SGS (Smagorinsky-type) model have shown no further improvement of the results. This agrees with the conclusion of [3] that when no explicit subgrid scale modelling is added, a high-resolution method will not add any unnecessary diffusion.

## 4. CONCLUDING REMARKS

Numerical experiments were conducted to investigate the accuracy and limitations of high-resolution schemes in ILES using the compressible Euler and Navier–Stokes equations. The results were found in good agreement with DNS and experimental data for the flow past an open, rectangular cavity. Reasonable results were also achieved in under-resolved simulations of decaying turbulence in a triply periodic cube. Less dissipative flux variants, e.g. the characteristics-based scheme, and more dissipative ones, e.g. the hybrid TVD scheme, were found to perform better in transonic and supersonic flows, respectively. Variants of different hybrid TVD schemes are currently under investigation.

 

ACKNOWLEDGEMENTS

The financial support from EPSRC, BAE SYSTEMS and MoD through the DARP consortium 'Modelling and Simulation of Turbulence and Transition for Aerospace' is greatly acknowledged. The authors would like to thank Fernando Grinstein and Piotr Smolarkiewicz for fruitful discussions on the problem of decaying turbulence.

REFERENCES

1. Boris JP, Grinstein FF, Oran ES, Kolbe RJ. New insights into large eddy simulation. *Fluid Dynamics Research* 1992; **10**:199–228.
2. Youngs DL. Three-dimensional numerical simulation of turbulent mixing by Rayleigh–Taylor instability. *Physics of Fluids* 1991; **3**:1312–1320.
3. Margolin LG, Smolarkiewicz PK, Sorbjan Z. Large eddy simulations of convective boundary layers using nonoscillatory differencing. *Physica D* 1998; **133**:390–397.
4. Grinstein F. Vortex dynamics and entrainment in rectangular free jets. *Journal of Fluid Mechanics* 2001; **437**:69–101.
5. Margolin LG, Rider WJ. A rationale for implicit turbulence modeling. *International Journal for Numerical Methods in Fluids* 2002; **39**:821–841.
6. Drikakis D. Embedded turbulence model in numerical methods for hyperbolic conservation laws. *International Journal for Numerical Methods in Fluids* 2002; **39**:763–781.
7. Smolarkiewicz PK, Prusa JM. VLES modeling of geophysical fluids with nonoscillatory forward-in-time schemes. *International Journal for Numerical Methods in Fluids* 2002; **39**:799–819.
8. Mallinger B, Drikakis D. Instability in three-dimensional, unsteady stenotic flows. *International Journal of Heat and Fluid Flow* 2002; **23**:657–663.
9. Fureby C, Grinstein FF. Large eddy simulation of high Reynolds number free and wall bounded flows. *Journal of Computational Physics* 2002; **181**:68–97.
10. Margolin LG, Smolarkiewicz PK, Wyszogrodzki AA. Implicit turbulence modeling for high Reynolds number flows. *Journal of Fluids Engineering* 2002; **124**:862–867.
11. Youngs DL. Application of MILES to Rayleigh–Taylor and Richtmyer–Meshkov mixing. *AIAA Paper 2003-4102*, 2003.
12. Drikakis D. Advances in turbulent flow computations using high-resolution methods. *Progress in Aerospace Sciences* 2003; **39**:405–424.
13. Drikakis D, Rider W. *High-Resolution Methods for Incompressible and Low-Speed Flows*. Springer: Berlin, 2004.
14. Shu CW, Osher S. Efficient implementation of essentially non-oscillatory shock-capturing schemes. *Journal of Computational Physics* 1988; **77**:439–471.
15. Zóltak J, Drikakis D. Hybrid upwind methods for the simulation of unsteady shock-wave diffraction over a cylinder. *Computer Methods in Applied Mechanics and Engineering* 1998; **162**:165–185.
16. Bagabir A, Drikakis D. Numerical experiments using high-resolution schemes for unsteady, inviscid, compressible flows. *Computer Methods in Applied Mechanics and Engineering* 2004; **193**(42–44):4675–4705.
17. Eberle A. Characteristic flux averaging approach to the solution of Euler's Equations. *Computational Fluid Dynamics*, VKI Lecture Series, *Report 1987-04*, 1987.
18. Herring JR, Kerr RM. Development of enstrophy and spectra in numerical turbulence. *Physics of Fluids A* 1993; **5**:2792–2798.
19. Porter DH, Pouquet A, Woodward PR. Kolmogorov-like spectra in decaying three-dimensional supersonic flows. *Physics of Fluids* 1994; **6**:2133–2142.
20. Rowley CW. Modeling, simulation, and control of cavity flow oscillations. *Ph.D. Thesis*, California Institute of Technology, 2002.
21. Zhang X. An experimental and computational investigation into shear layer driven single and multiple cavity flowfields. *Ph.D. Thesis*, University of Cambridge, 1988.

 